https://doi.org/10.15360/1813-9779-2022-2-22-36

Metabolomic Profiling of the Blood of Patients with Chronic Disorders of Consciousness

Anastasia A. Orlova[1], Ekaterina A. Kondrat'eva[2,3]*, Yaroslav A. Dubrovskii[4], Natalia V. Dryagina[2], Elena V. Verbitskaya[5], Sergey A. Kondratev[2], Anna A. Kostareva[4], Anatoly N. Kondratev[2]

[1] St. Petersburg State Chemical and Pharmaceutical University, Ministry of Health of Russia, 14 Professor Popova Str., 197376 St. Petersburg, Russia
[2] A. L. Polenov Russian Research Institute for Neurosurgery, V.A. Almazov National Research Center, 12 Mayakovsky Str., 191014 St. Petersburg, Russia
[3] Federal Research and Clinical Center of Intensive Care Medicine and Rehabilitology, 25 Petrovka Str., Bldg. 2, 107031 Moscow, Russia
[4] V. A. Almazov National Medical Research Center, Ministry of Health of Russia, 2 Akkuratova Str., 197341 St. Petersburg, Russia
[5] Academician I. P. Pavlov First Saint-Petersburg State Medical University, Ministry of Health of Russia, 6–8 Lev Tolstoy Str., 197022 St. Petersburg, Russia

For citation: *Anastasia A. Orlova, Ekaterina A. Kondrat'eva, Yaroslav A. Dubrovskii, Natalia V. Dryagina, Elena V. Verbitskaya, Sergey A. Kondratev, Anna A. Kostareva, Anatoly N. Kondratev.* Metabolomic Profiling of the Blood of Patients with Chronic Disorders of Consciousness. *Obshchaya Reanimatologiya = General Reanimatology.* 2022; 18 (2): 22–36. http://doi.org/10.15360/1813-9779-2022-2-22-36 [In Russ. and Engl.]

Summary

The main variants of chronic disorders of consciousness (cDoC) developing in adverse coma outcome are vegetative state/unresponsive wakefulness syndrome (VS/UWS) and minimal consciousness state (MCS).

The aim of the study was to investigate the main differences in metabolomic abnormalities in patients with VS/UWS and MCS, as well as to identify changes in metabolomics depending on sleep or wakefulness phase.

Materials and Methods. Untargeted metabolome analysis of blood plasma of 10 patients in VS/UWS (group 1) and 6 patients in MCS (group 2) was performed using reversed-phase and hydrophilic chromatography methods. The underlying conditions of brain injury were TBI (2 in group 1 and 5 in group 2) and hypoxia (8 in group 1 and 1 in group 2). The internal jugular vein was catheterized in all patients, and blood was collected while awake during the daytime for 2 days. Aliquots of pooled plasma samples were purified from protein components and analyzed by high-performance liquid chromatography in two modes: reversed-phase and hydrophilic ones. Mass-spectrometric detection was performed in full ion current scanning mode: registration of positively charged ions in the m/z range from 50 to 1300 a.u. Data were adjusted and normalized using MS-DIAL software ver. 4.70 software; differences were identified using analysis of variance, discriminant and cluster analysis. The data were analyzed and visualized using MetaboAnalyst 5.0 software (https://www.metaboanalyst.ca).

Results. Four major metabolites (at VIP > 0.5), which content was most modulated depending on the study group, were identified including 4 (*m/z* 124.0867, Rt=17.67, $p<0.01$), 33 (*m/z* 782.5722, *Rt*=17.69, $p<0.01$), 6 (*m/z* 125.0904, *Rt*=18.43, $p<0.01$) and 1 (*m/z* 463.2304, *Rt*=15.78, $p<0.01$), with no significant differences between daytime and nighttime blood samples. Significant quantitative differences were shown for three metabolites in the groups, 14 (*m/z* 162.1126, *Rt*=10.28, $p<0.01$), 35 (*m/z* 780.5483, *Rt*=7.65, $p<0.01$), and 41 (*m/z* 806.5649, *Rt*=7.58, $p<0.01$), and four metabolites when comparing the daytime and nighttime samples: 14 (*m/z* 162.1126, *Rt*=10.28, $p=0.0201$), 35 (*m/z* 780.5483, *Rt*=7.65, $p<0.01$), 41 (*m/z* 806.5649, *Rt*=7.58, $p<0.01$), and 48 (*m/z* 848.5354, *Rt*=7.65, $p<0.01$).

Conclusion. Untargeted metabolomic analysis confirmed the hypothesis of likely significant quantitative and qualitative differences in metabolite composition depending on the type of CCD and circadian rhythm. The study established a set of metabolites that are potential biomarkers for differential diagnosis of VS/UWS and MCS including 4, 33, 6, 1 (in the experiment on the reversed-phase column) and 14, 35, 41, 48 (in the experiment on the hydrophilic column), based on their significant contribution to intergroup and intragroup differences. Further studies will be aimed to characterize the identified metabolites.

Keywords: chronic disorders of consciousness; vegetative state; unresponsive wakefulness syndrome; minimal consciousness state; metabolomics; metabolomic profile; blood-brain barrier; circadian rhythm; glymphatic system; prediction of consciousness recovery; multidisciplinary approach

Funding. The study was supported by the Russian Foundation for Basic Research under Scientific Project No. 19-29-01066.

Conflict of Interest. The authors declare no conflict of interest.

Correspondence to:

Ekaterina A. Kondratieva
E-mail: eak2003@mail.ru

Адрес для корреспонденции:

Екатерина Анатольевна Кондратьева
E-mail: eak2003@mail.ru

Introduction

Chronic disorders of consciousness (cDoC) include variants of adverse coma outcomes, when a patient exhibits no or severe signs of impaired consciousness [1]. The main forms of cDoC include the «vegetative state» or «unresponsive wakefulness syndrome» (VS/UWS), when there is lack of self-awareness and awareness of the environment along with the preserved sleep-wake cycle, as well as the «minimally conscious state minus», when the patient is available for a minimal contact, i. e., visual fixation and eye tracking are present, and a «minimally conscious state plus», when the patient is able to perform a simple task and answer a «yes-no» question verbally or by nodding [2–4].

Significant progress has been made in recent decades in understanding the mechanisms of impaired consciousness after severe brain damage, and a multidisciplinary approach to this problem has been described as a way to bridge the gaps for advancing toward integrated translational science [5]. The most studied and stable functional states of the brain are sleep and wakefulness which occur in circadian rhythms. The study of sleep structure in patients with cDoC becomes particularly relevant due to the discovery of the brain's glymphatic system, which allows the removal of amyloid proteins and tau-oligomers from the glia during the slow sleep phase [6]. Impaired functioning of this system is one of the mechanisms for the development of neurodegenerative processes and neuroinflammation [7–9]. In our opinion, the study of sleep and wake processes in patients with cDoC is particularly interesting from the viewpoint of studying the functional state of the brain, as well as the homeostasis regulation variants supporting these phases. In this respect, metabolomics can be considered as one of the approaches to reveal potential low-molecular-weight biomarkers of the brain performance in patients with cDoC. The general metabolomic profile can serve as a direct indicator of metabolic changes in a biological system [10]. The blood-brain barrier (BBB) is known to be impermeable to most metabolites under normal conditions. Various pathological conditions such as neurodegeneration, neuroinflammation, traumatic brain injury (TBI), and hypoxia result in disruption of the BBB, functioning in both directions; hence, the plasma metabolomic profile may reflect metabolic disorders in the brain [11, 12]. Changes in blood metabolome profile in stroke [13], traumatic brain injury [14], diabetes mellitus [15], and cancer [16–18] have been actively studied.

Analysis of metabolomic research results obtained in the study of sleep and wake phases in patients with cDoC should make it possible to identify additional prognostic markers of potential recovery of consciousness and develop pathogenetic approaches to the treatment of this category of patients in the future. Thus, the aim of this study was to investigate the main differences in metabolomic disorders in patients in the vegetative state/unresponsive wakefulness syndrome and minimally conscious state and identify changes in the metabolome depending on sleep or wake phase.

Material and Methods

The study was supported by the ethical committee of the V. A. Almazov Scientific Research Center (protocol No. 23082019) and was conducted in accordance with the Code of Ethics of the World Medical Association (Declaration of Helsinki). Patients stayed in the anesthesiology and intensive care unit for at least 21 days (in 2019–2020). Sixteen patients with cDoC were included in the study. To evaluate the signs of consciousness, the patients were assessed on the Coma Recovery Scale- Revised (CRS-R) 5 times during the first 10 days of hospitalization. Depending on the total CRS-R score, patients were divided into two groups. Group 1 included patients with a CRS-R score of 0 to 5 (their level of consciousness met the VS/UWS criteria), and Group 2 included patients with a CRS-R score of 9 to 15 (their level of consciousness met the MCS «minus» or «plus» criteria). Characteristics of patients by age, duration of consciousness disorder, and total CRS-R score are shown in Table 1.

The causes of brain damage included TBI (2 in group 1 and 5 in group 2) and hypoxia (8 in group 1 and 1 in group 2). Patients with acute infection, hepatic and renal dysfunction were not included in the study. Medications received by the patients at the time of serum sampling are presented in Table 2.

The study steps are shown in Fig. 1.

A catheter was inserted into the right jugular vein in all patients a day before the examination, with the catheter tip directed upward (against the blood flow) — to obtain blood «flowing out» from the brain. Blood sampling was performed in the awake state at daytime (at 12:00) and at night (at 3:00 am) for 2 days (two daytime and two nighttime samplings were performed for 2 days). Blood was collected in vacutainers with EDTA as an anticoagulant, placed on ice, and immediately taken to the laboratory, where it was centrifuged for 15 minutes at 2700 rpm, aliquoted in Eppendorf tubes, and frozen at –25°C. Hemolyzed samples were discarded and not included in further study.

Preparation of samples. Pooling and purification of blood plasma from protein molecules. Pooled blood plasma samples were used for analysis. Pools were formed at the daytime and nighttime points for each group, i.e., 2 pooled

https://doi.org/10.15360/1813-9779-2022-2-22-36

Table 1. Characteristics of patients with chronic disorders of consciousness.

Main parameters	Age, years	Duration of disorder of consciousness, months	CRS, points
Group 1 (*n*=10)			
Mean	38	5.4	4
Standard deviation	12	7.8	1
Median	40	2.0	4
Minimum	21	1.0	1
Maximum	54	26.0	5
25th percentile	26	1.0	3
75th percentile	45	6.0	5
Group 2 (*n*=6)			
Mean	37	9.7	12
Standard deviation	15	11.3	2
Median	31	4.0	11
Minimum	21	1.0	9
Maximum	61	26.0	15
25th percentile	29	1.0	10
75th percentile	51	22.0	13

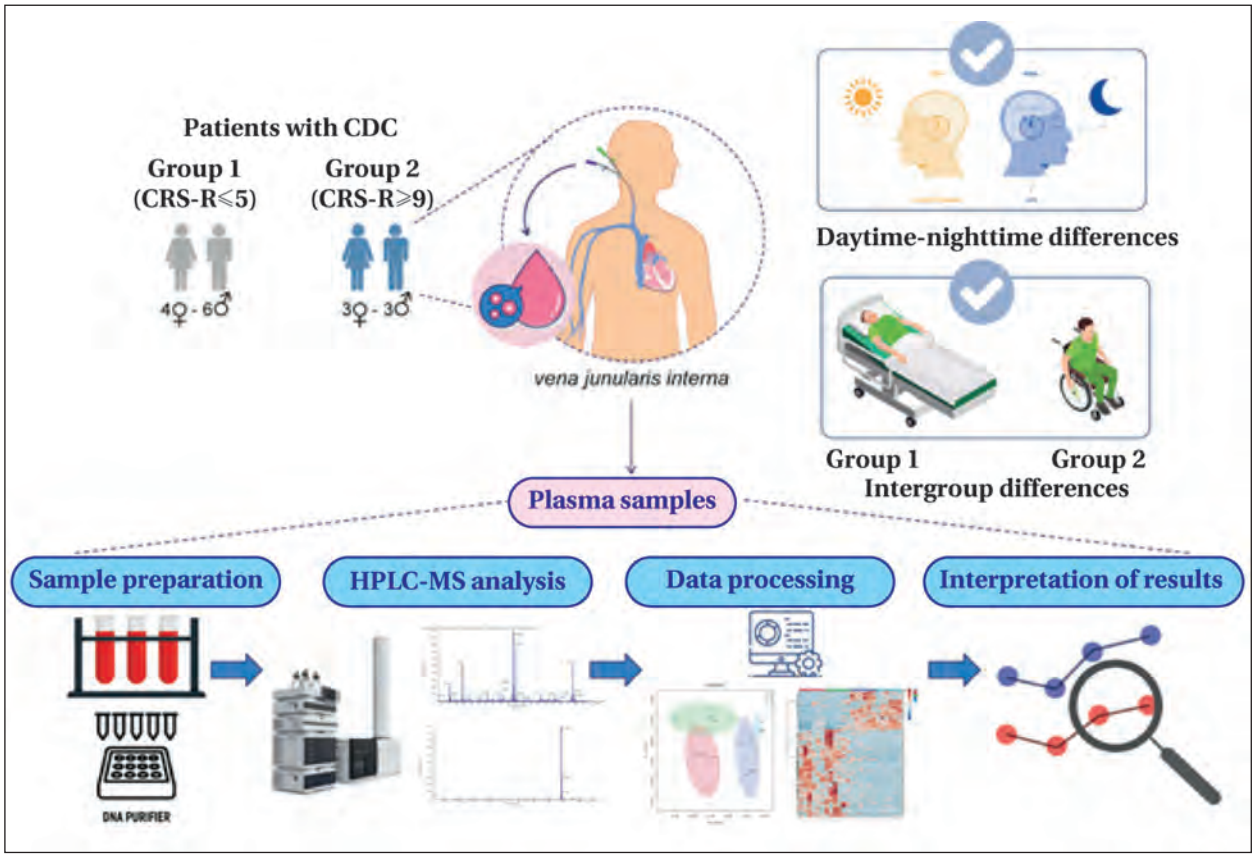

Fig. 1. The steps of the non-targeted blood test in patients with chronic disorders of consciousness.

samples were formed in Group 1 (daytime sample contained the plasma of 10 patients of first and second day sampling; nighttime sample contained the plasma of 10 patients of first and second nighttime sampling) and 2 pooled samples in Group 2 (daytime sample contained the plasma of 6 patients of first and second daytime sampling; nighttime sample contained the plasma of 6 patients of first and second nighttime sampling). An aliquot of 100 μL was taken from each pooled sample and transferred to a new Eppendorf tube. Then, 400 μl of chilled acetonitrile was added to each sample and stirred. To remove protein components, samples were centrifuged for 10 min (12,000 rpm, 4°C), and 400 μl of supernatant was transferred to a chromatographic vial for subsequent analysis.

Chromatography and mass spectrometry. Conditions of chromatographic separation. The chromatographic separation of the components

Table 2. List of medications received by patients from the study groups.

Group 1 (VS/UWS)	Group 2 (MCS)
Ipidacrine	
Amlodipine	
Bisoprolol	
Valproic acid	
Phenytoin	
Ethylmethylhydroxypyridine succinate	
Amantadine sulfate	
Nadroparin calcium	
Tolperisone hydrochloride	
Choline alfoscerate	
Citicoline	
Omeprazole	
Spironolactone	Lactulose
Levetiracetam	Clonidine
Memantine	Proroxan
Pancreatin	Brain peptide complex
Carbamazepine	
Fluconasole	
Succinic acid, inosine, nicotinamide	
Apixaban	
Levothyroxine	

Table 3. Ratio of mobile phase components.

Time, minutes	A,%	B,%
0	95	5
0.5	95	5
15.5	45	55
16.5	25	75
17.5	25	75
17.6	95	5
20	95	5

Note. Eluent flow rate = 0.3 ml/min; column thermostat temperature = 40°C; thermostat temperature (sampling department) = 10°C; sample injection volume — 2 µl; analysis time — 20 min.

Table 4. Ratio of mobile phase components.

Time, minutes	A,%	B,%
0	5	95
3	5	95
12	40	60
15	40	60
16	5	95
20	5	95

Note. Eluent flow rate = 0.3 ml/min; column thermostat temperature = 40°C; thermostat temperature (sampling department) = 10°C; sample injection volume — 2 µl; analysis time — 20 min.

using high-performance liquid chromatography (HPLC) was performed in two modes:

1. Reverse phase chromatography

- Intensity Solo 2 C18 (Bruker) column, length 100 mm, column diameter 2.10 mm, sorbent particle diameter 1.8 µm.
- The mobile phase:
  - component A — 0.1% solution of formic acid in deionized water;
  - component B — HPLC category acetonitrile;
- Gradient chromatographic elution mode

Hydrophilic interaction liquid chromatography (HILIC)

- Ascentis Express HILIC (Merck) column, length 100 mm, column diameter 2.10 mm, diameter of sorbent particles 2.7 µm
- Mobile phase:
  - component A — 10 mM NH4COOH with added formic acid (0.1%) in deionized water;
  - component B — HPLC category acetonitrile;
- Gradient chromatographic elution mode

Operating conditions of the mass spectrometric detector. Mass spectrometric detector was Bruker Q-TOF Maxis Impact with electrospray ionization at atmospheric pressure and «otof Control» software for data control and processing.

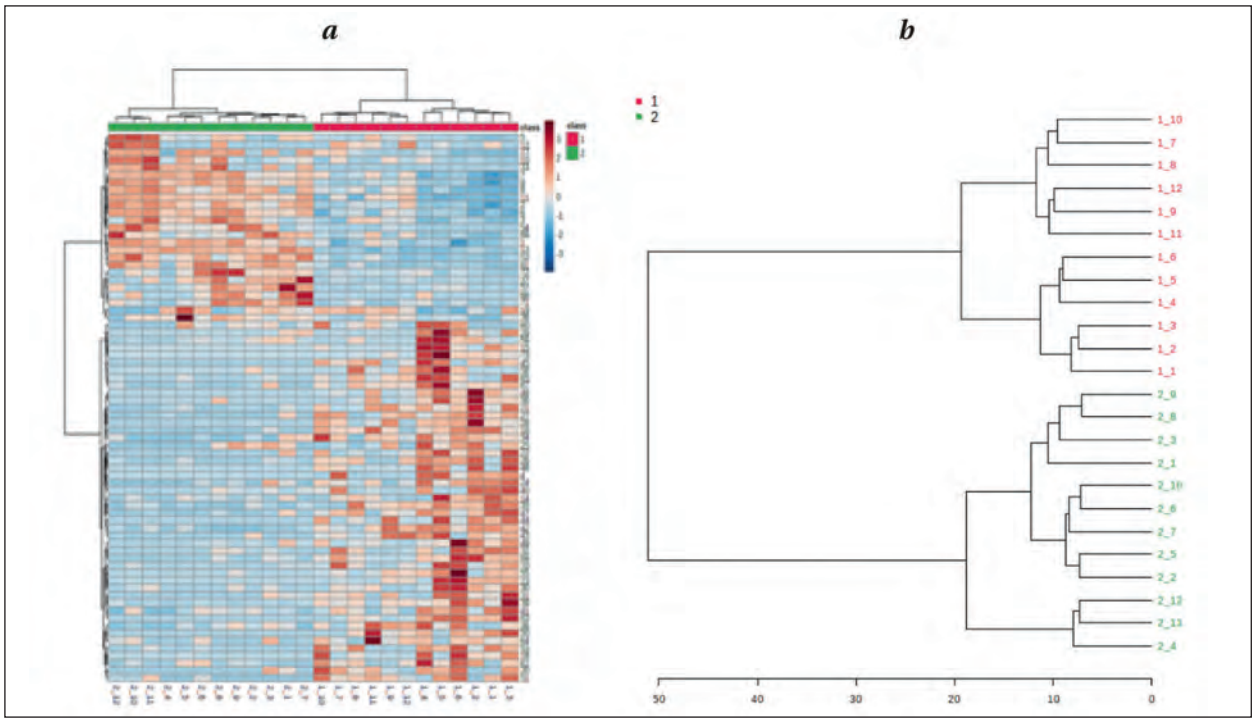

Fig. 2. Hierarchical cluster analysis of samples from groups 1 and 2 from the C18 column.
Note. *a* — heat map of metabolites. The studied plasma samples by groups are arranged in columns: red correspond to group 1, green to group 2, and the identified component variables are arranged in rows. The colors range from blue to red, indicating a change in the content of the variables from very low (dark blue) to high (dark red). *b* — dendrogram. Samples form clusters of groups 1 (red) and 2 (green).

Mode: drying gas flow (nitrogen) 8 l/min; gas pressure on the nebulizer 2 bar; conducting capillary temperature 220°C; capillary voltage 4500 V; detection in full ionic current scanning mode: registration of ions in the m/z range from 50 to 1300 a.u. (with positive ionization).

Data processing. Data from the chromatomass spectrometric analysis were converted to mzML format and processed using MS-DIAL metabolomics software (http://prime.psc.riken.jp/Metabolomics_Software/MS-DIAL/index.html). Data adjustment, normalization, and filtering (the data were cleared of background noise and unrelated ions) were performed using MS-DIAL software ver. 4.70. The concentrations of the studied substances by definition have a log-normal distribution, so the data were subjected to median normalization, logarithmic transformation, and automatic scaling (centeraveraged and divided by the standard deviation of each variable). Data were statistically processed and visualized using the MetaboAnalyst 5.0 platform (https://www.metaboanalyst.ca/), which is generally accepted for metabolic analysis. The intergroup differences were tested using Student's test, Mann-Whitney test (to compare groups 1 and 2), and ANOVA test (to compare circadian changes of metabolomics) in accordance with normally distributed logarithmically transformed variables. The critical level of significance was set at α=0.05. In addition, we performed unsupervised principal component analysis (PCA) and supervised PLS-DA analysis with a Pareto-scaled data set and power transformation using the first two latent variables. Based on the PLS-DA models, we created volcano plots showing the importance of variables in projection (VIP) versus adjusted p-values [p (corr), load values scaled as correlation coefficient values]. Variables with VIP > 0.5, q ⩽ 0.050, and absolute p (corr) ⩾ 0.30 were considered significant. To illustrate complex associations between several parameters based on normalized data, cluster analysis was performed, in which clustering was performed using the Ward method, and the Euclidean distance was considered as a measure of proximity [19, 20].

Results

Initial data processing. Pooled blood samples from cDoC patients of two groups were analyzed. High-performance liquid chromatography with mass spectrometry detector (HPLC-MS) data for all pooled samples were obtained on two different chromatographic columns, hydrophilic (HILIC) and reversed-phase (C18), for comprehensive evaluation of metabolites of different polarity. Group spectra

showed a consistent set of metabolite signals present. The number of raw spectral signals detected instrumentally was 6569 for HILIC analysis and 7952 on the C18 column. Noise and artifact peaks were filtered out, yielding 6134 and 4759 signals, respectively. Based on the hypothesis of probable significant quantitative and qualitative differences in the composition of metabolites depending on the severity of patient condition, we identified those metabolites whose relative levels, calculated from chromatographic peak areas, dempnstrated significant intergroup differences, using ANOVA analysis. Thus, we identified 63 metabolites for the HILIC column and 73 metabolites for the C18 column (P<0.05) (Table 5, 6 — see Appendix).

Analysis of reversed-phase chromatography data. Normalized data of the relative intensities of the chromatographic signals obtained on the C18 column were imported into MetaboAnalyst 5.0 software and visualized using cluster analysis techniques. The resulting hierarchically grouped heat map of metabolites reflects a comparative assessment of mean metabolite contents, and the dendrogram demonstrates, on the one hand, a significant correlation between all samples from one group, and a distinct clustering of samples belonging to groups 1 and 2 on the other hand (Fig. 2).

Preliminary conclusions were confirmed using other statistical methods. An estimation plot based on the unsupervised PCA model (Fig. 3, *a*) showed clusters of Group 1 (VS/UWS) and Group 2 (MCS) samples in the two main components PC1 and PC2, which accounted for 87% and 12% of the variance in the data, respectively. To make this difference more apparent, we performed a supervised PLS-DA analysis with a Pareto-scaled data set and power transformation using the first two latent variables. This model produced clusters similar to the PCA for groups 1 and 2 (Fig. 3, *b*), and both models showed relatively greater homogeneity of group 2 samples. According to the PLS-DA loading plots (Fig. 3, *c*), we identified four major metabolites (at VIP > 0.5) whose content was most modulated depending on the patient group, which included signal 4 (m/z 124.0867, Rt=17.67, P<0.01), 33 (m/z 782.5722, Rt=17.69, P<0.01), 6 (m/z 125.0904, Rt=18.43, P<0.01), and 1 (m/z 463.2304, Rt=15.78, P<0.01). Metabolite 4 content was higher in group 1, while the content of metabolites 33, 6, and 1 was higher in group 2.

When analyzing differences in the composition of metabolites of daytime and nighttime samples on column C18, no significant differences were found. Hierarchical cluster analysis showed a significant correlation between both daytime and nighttime samples of the same group (Fig. 4, *a* and *b*), no isolated clusters of daytime and nighttime sampling appeared in the PLS-DA analysis (Fig. 5).

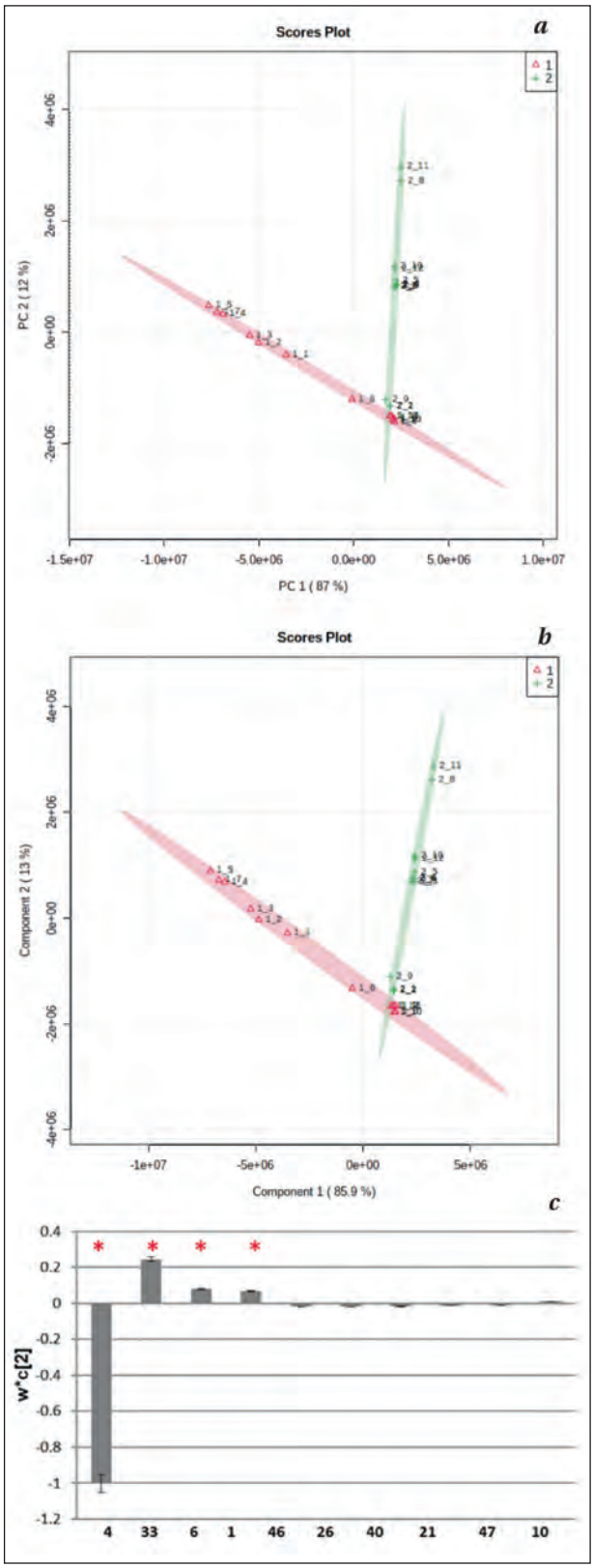

Fig. 3. Graphs of the assessment of PCA (A) and PLS-DA (B) in groups 1 and 2 from C18 column.
Note. In Figures *a* and *b*, the red cloud represents the cluster of group 1, the green one — the cluster of group 2. 1_1-1_12 — studied plasma samples from patients of group 1; 2_1-2_12 — studied plasma samples from patients of group 2. *b* — PLS-DA model load graph observed by PC 2 (w * c [2]): each column represents a putative marker metabolite with standard errors displayed in the error bar.

Table 5. List of target metabolites for the HILIC column

Metabolite No.	m/z	tR	Normalized mean for group 1	Normalized mean for group 2	*P* value
1	116.07095	2.488	0.723±0.626	–0.723±0.747	<0.0001*
2	121.96481	8.845	0.730±0.221	–0.730±0.938	0.0002*
3	129.06573	9.348	0.800±0.507	–0.800±0.662	<0.0001*
4	129.97771	10.045	–0.549±1.025	0.549±0.617	0.0018**
5	131.95901	8.258	–0.209±0.593	0.209±1.282	0.0284**
6	133.95724	8.564	–0.864±0.569	0.864±0.374	<0.0001*
7	136.04131	3.363	0.038±1.257	–0.038±0.712	0.3777**
8	143.99974	10.047	–0.607±1.100	0.607±0.275	0.0028*
9	144.98315	6.978	–0.766±0.891	0.766±0.129	<0.0001*
10	146.1156	10.44	–0.275±0.971	0.275±0.991	0.1842*
11	146.11641	10.411	–0.265±0.972	0.265±0.996	0.2005*
12	153.03342	9.78	–0.766±0.859	0.766±0.271	<0.0001**
13	156.04485	9.013	–0.908±0.463	0.908±0.278	<0.0001*
14	162.11261	10.278	0.206 ±0.778	–0.206±1.180	0.3228*
15	175.11806	10.621	–0.823±0.557	0.823±0.552	<0.0001*
16	185.02979	1.43	–0.012±0.954	0.012±1.086	0.955*
17	188.07005	7.322	–0.408±0.695	0.408±1.116	0.0427*
18	226.04523	7.582	–0.478±0.821	0.478±0.958	0.0155*
19	353.07663	3.476	–0.695±0.381	0.695±0.944	0.0003*
20	385.03558	7.325	0.075±0.898	–0.0750±0.128	0.2657**
21	480.34351	8.566	–0.853±0.482	0.853±0.520	<0.0001*
22	496.62271	8.726	0.369±0.221	–0.369±1.321	0.0284**
23	533.32251	3.401	0.369±0.623	–0.369±1.186	0.0145**
24	566.89081	7.513	–0.860±0.584	0.860±0.370	<0.0001*
25	634.87213	7.513	–0.899±0.398	0.899±0.413	<0.0001*
26	701.49713	7.245	–0.898±0.468	0.898±0.333	<0.0001*
27	702.85931	7.513	–0.884±0.428	0.884±0.452	<0.0001*
28	736.86053	7.512	–0.879±0.431	0.879±0.469	<0.0001*
29	738.50195	6.442	0.473±0.087	–0.473±1.263	0.0029**
30	741.53412	8.296	–0.884±0.471	0.884±0.407	<0.0001*
31	759.04663	7.651	0.663±0.486	–0.663±0.946	0.0005*
32	759.17041	7.65	0.523±0.794	–0.523±0.929	0.0071*
33	769.55829	7.652	–0.773±0.694	0.773±0.553	<0.0001*
34	770.85394	7.513	–0.884±0.444	0.884±0.434	<0.0001*
35	780.54828	7.654	–0.873±0.515	0.873±0.403	<0.0001**
36	784.93988	7.592	0.642±0.373	–0.642±1.026	0.0012*
37	786.96295	7.596	0.236±1.240	–0.236±0.657	0.2593*
38	793.54767	8.297	–0.901±0.457	0.901±0.333	<0.0001*
39	796.54877	7.777	–0.812±0.611	0.812±0.527	<0.0001*
40	802.58978	1.545	–0.017±1.071	0.017± 0.971	0.936*
41	806.56488	7.584	–0.823±0.593	0.823±0.510	<0.0001*
42	814.55292	7.813	–0.741±0.906	0.741±0.268	<0.0001**
43	815.54834	7.522	0.556±0.475	–0.556±1.091	0.0055*
44	818.52917	7.645	–0.655±1.040	0.655±0.271	<0.0001**
45	818.59137	7.579	0.101±0.874	–0.101±1.143	0.9774**
46	833.64746	8.141	0.255±1.098	–0.255±0.862	0.1005**
47	843.57544	7.474	–0.878±0.505	0.878±0.392	<0.0001*
48	848.5354	7.654	0.831±0.473	–0.831±0.602	<0.0001*
49	852.55658	5.647	0.456±0.413	–0.456±1.211	0.0100**
50	854.55298	7.578	0.257±0.569	–0.257±1.274	0.5899**
51	856.5672	7.58	–0.299±1.197	0.299±0.681	0.1473*
52	862.54602	7.497	–0.949±0.272	0.949±0.223	<0.0001*
53	867.07965	7.481	0.286±0.545	–0.286±1.271	0.5137**
54	868.52759	7.404	–0.827±0.555	0.827±0.537	<0.0001*
55	874.5517	7.581	0.644±0.383	–0.644±1.020	0.0011*
56	876.55682	5.555	–0.892±0.465	0.892±0.370	<0.0001**
57	876.57294	7.59	0.552±0.457	–0.552±1.103	0.0002**
58	878.56982	5.604	–0.112±1.418	0.112±0.228	0.1432**
59	880.58649	5.616	0.121±0.765	–0.121±1.214	0.8874**
60	896.56024	7.365	–0.868±0.454	0.868±0.489	<0.0001*
61	906.8288	7.513	–0.203±0.888	0.203±1.101	0.3307*
62	922.5542	7.445	–0.879±0.433	0.879±0.468	<0.0001*
63	974.80841	7.513	0.723±0.626	–0.723±0.747	<0.0001*

Note. Here and in Table 6: * — *P* value calculated using Student's *t*-test; ** — *P* value calculated using the Mann–Whitney test.

Table 6. List of target metabolites for the C18 column.

Metabolite No.	m/z	tR	Normalized mean for group 1	Normalized mean for group 2	*P* value
1	15.78	463.2304	–0.755±0.768	0.755±0.506	<0.0001**
2	18.65	108.0811	–0.798±0.485	0.798±0.684	<0.0001*
3	18.77	118.0872	–0.708±0.912	0.708±0.406	<0.0001**
4	17.67	124.0867	–0.257±1.062	0.257±0.905	0.3777*
5	17.93	124.1716	–0.692±0.639	0.692±0.799	0.0001*
6	18.43	125.0904	–0.803±0.665	0.803±0.493	<0.0001*
7	18.78	128.9628	–0.753±0.757	0.753±0.529	<0.0001*
8	19.05	131.9308	–0.711±0.884	0.711±0.453	<0.0001**
9	18.71	131.9625	–0.812±0.518	0.812±0.620	<0.0001*
10	17.75	138.102	–0.671±0.725	0.671±0.764	0.0002*
11	18.71	147.0929	–0.731±0.888	0.731±0.369	0.0001*
12	18.82	182.9617	–0.357±0.820	0.357±1.068	0.1005**
13	18.77	90.5081	–0.883±0.422	0.883 ±0.460	<0.0001*
14	18.7	674.4291	–0.004±1.151	0.004±0.876	0.7728**
15	18.72	686.6918	0.404±1.271	–0.404±0.344	0.5443**
16	18.68	711.7711	0.675 ±0.727	–0.675±0.753	0.0007**
17	18.72	716.5522	–0.705±0.826	0.705±0.570	<0.0001*
18	17.75	723.4638	0.341±1.234	–0.341±0.561	0.4356**
19	18.54	727.4619	–0.622±0.764	0.622±0.814	0.0008*
20	18.66	727.7125	0.159 ±1.178	–0.159±0.806	0.3863**
21	18.66	738.4745	0.488 ±0.581	–0.488±1.111	0.0156*
22	18.72	741.2301	0.636±0.899	–0.636±0.632	0.0262**
23	18.65	748.7361	0.290±1.240	–0.290 ±0.608	0.3122**
24	17.73	755.4784	0.519±0.581	–0.519±1.080	0.0376**
25	17.78	757.9766	–0.250±1.040	0.250±0.935	0.2288*
26	17.72	763.49	0.286±1.041	–0.286± 0.911	0.1409**
27	18.63	772.2356	0.530±0.749	–0.530±0.957	0.0193**
28	17.56	772.4897	0.551±1.029	–0.551±0.608	0.0056**
29	18.71	772.493	–0.010 ±1.187	0.010±0.825	0.5066**
30	18.7	773.4938	0.043±1.031	–0.043±1.012	0.8852**
31	18.71	778.0045	0.345 ±1.088	–0.345±0.804	0.0734**
32	17.93	778.9939	0.210±1.166	–0.210±0.797	0.4095**
33	17.69	782.5722	–0.790±0.725	0.790±0.452	<0.0001**
34	18.7	782.7464	0.418±0.530	–0.418±1.195	0.1600**
35	17.9	792.5078	0.375±0.663	–0.375±1.160	0.0646*
36	18.71	793.3143	0.068±1.002	–0.068±1.037	0.7475*
37	18.67	800.6866	–0.755±0.662	0.755±0.639	<0.0001*
38	17.91	802.0062	–0.777±0.573	0.777±0.667	<0.0001*
39	17.66	805.7479	0.457±0.630	–0.457±1.113	0.0209**
40	17.8	808.5083	0.026±1.215	–0.026±0.784	0.8874**
41	18.64	813.5074	–0.108±0.921	0.108±1.103	0.6085*
42	17.95	816.5212	0.325±0.392	–0.325±1.306	0.1224*
43	17.65	821.1963	0.532±0.836	–0.532±0.880	0.0145**
44	17.93	821.8597	0.692±0.936	–0.692±0.410	0.0003*
45	17.7	829.8372	0.669±0.958	–0.669±0.442	0.0043**
46	17.79	831.8625	0.566±1.008	–0.566±0.613	0.0031*
47	18.67	831.863	0.470±0.869	–0.470±0.923	0.0145**
48	17.76	848.8497	0.589±1.037	–0.589±0.507	0.0028*
49	17.89	849.0341	0.293±0.961	–0.293±0.990	0.1550*
50	18.7	855.7933	0.257±1.180	–0.257±0.744	0.2151*
51	18.71	857.2792	0.379±0.753	–0.379±1.100	0.2144**
52	18.62	862.7601	–0.858±0.582	0.858±0.384	<0.0001*
53	18.58	863.1935	0.401±1.020	–0.401±0.837	0.1938**
54	18.66	867.7538	–0.747±0.616	0.747±0.703	0.0002**
55	18.63	877.3093	0.546±0.906	–0.546±0.787	0.0086**
56	17.87	886.5561	0.374±1.072	–0.374±0.798	0.1135**
57	18.63	887.5426	–0.826±0.445	0.826±0.637	<0.0001**
58	18.64	896.2261	–0.008±1.236	0.008±0.751	0.7125**
59	17.83	897.5506	–0.119±0.990	0.119±1.039	0.5726*
60	18.65	915.5733	–0.012±1.010	0.012±1.034	0.6297**
61	18.71	919.8516	–0.814±0.762	0.814±0.259	<0.0001*
62	18.57	926.2381	0.168 ±0.949	–0.168±1.062	0.6033**
63	18.69	928.9295	0.581±1.026	–0.581±0.548	0.0086**
64	17.96	935.5851	0.221±0.951	–0.221±1.039	0.5137**
65	17.64	935.9096	0.547±0.637	–0.547±1.016	0.0121**
66	18.64	948.9295	–0.853±0.402	0.853±0.583	<0.0001**
67	17.99	950.2549	0.634±0.228	–0.634±1.078	0.0018*
68	18.71	977.2341	–0.792 ±0.719	0.792±0.453	<0.0001*
69	18.65	982.1268	0.572±0.711	–0.572±0.934	0.0027*
70	18.63	1007.1024	0.398±1.014	–0.398 ±0.846	0.0605**
71	17.79	1033.6344	–0.835±0.665	0.835±0.356	<0.0001*
72	18.57	1036.2665	–0.736±0.804	0.736±0.513	<0.0001**
73	17.79	1056.1636	0.249±1.217	–0.249±0.690	0.2306*

https://doi.org/10.15360/1813-9779-2022-2-22-36

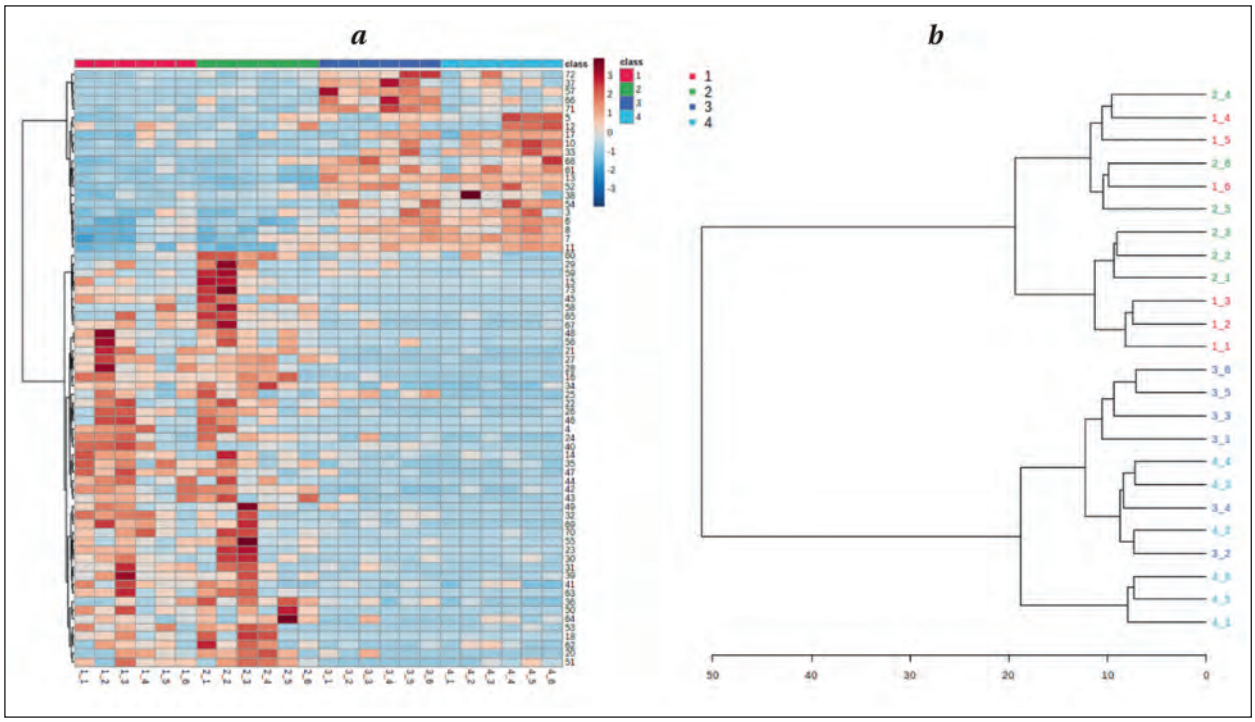

Fig. 4. Hierarchical cluster analysis of samples of daytime and nighttime sampling in the studied groups from C18 column.
Note. *a* — heat map of metabolites. The studied plasma samples are arranged by groups in the columns: red correspond to daytime sampling from group 1, green — nighttime sampling from group 1; dark blue — daytime sampling from group 2, blue — nighttime sampling from group 2, and the identified component variables are arranged in rows. The colors range from blue to red, indicating a change in the content of the variables: from very low (dark blue) to high (dark red). *b* — dendrogram: 1 — group 1, daytime sampling; 2 — group 1, nighttime sampling; 3 — group 2, daytime sampling; 4 — group 2, nighttime sampling. The samples form clusters of groups 1 and 2, but do not show a distinct clustering into daytime and nighttime sampling.

Analysis of hydrophilic chromatography data. The hierarchically grouped heat map of the metabolites with the highest relative content of the chromatographic signals obtained on the HILIC column and the dendrogram shows results similar to those obtained on the C18 column. All samples of the same group showed a significant correlation between each other when separating groups 1 and 2 into separate clusters (Fig. 6, *a, b*). However, when analyzing the data from the samples taken at different times, we observed them forming separate clusters indicating the presence of significant differences in the metabolic profiles of daytime and nighttime samples (Fig. 6, *c, d*).

The PCA and PLS-DA assessment plots showed distinct clustering of groups 1 and 2 in the two major components PC1 and PC2, which accounted for 99% and 0.5% of sample variance in PCA analysis (Fig. 7, *a*) and 99% and 0.3% in PLS-DA analysis (Fig. 7, *b*). The PLS-DA loading plots (Fig. 7, B) identified three major metabolites (at VIP > 0.5) most significant for clustering groups in the PLS-DA model, namely 14 (m/z 162. 1126, *Rt*=10.28, p < 0.01), 35 (m/z 780.5483, *Rt*=7.65, *P*<0.01), and 41 (m/z 806.5649, *Rt*=7.58, *P*<0.01), whose content was higher in group 1. When comparing daytime and nighttime sampling, however, there was marked

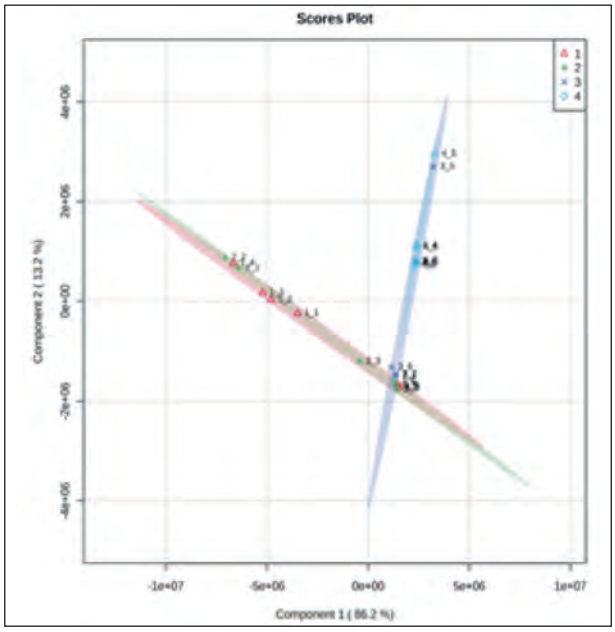

Fig. 5. PLS-DA analysis of differences between samples 1 and 2 with the daytime and nighttime sampling from C18 column.
Note. Red cloud represents group 1, daytime sampling; green cloud is group 1, nighttime sampling; dark blue cloud is group 2, daytime sampling; blue cloud is group 2, nighttime sampling. Red and green, dark blue and blue clouds overlap in pairs, which indicates the presence of intergroup and the absence of intragroup differences depending on the time of collection.

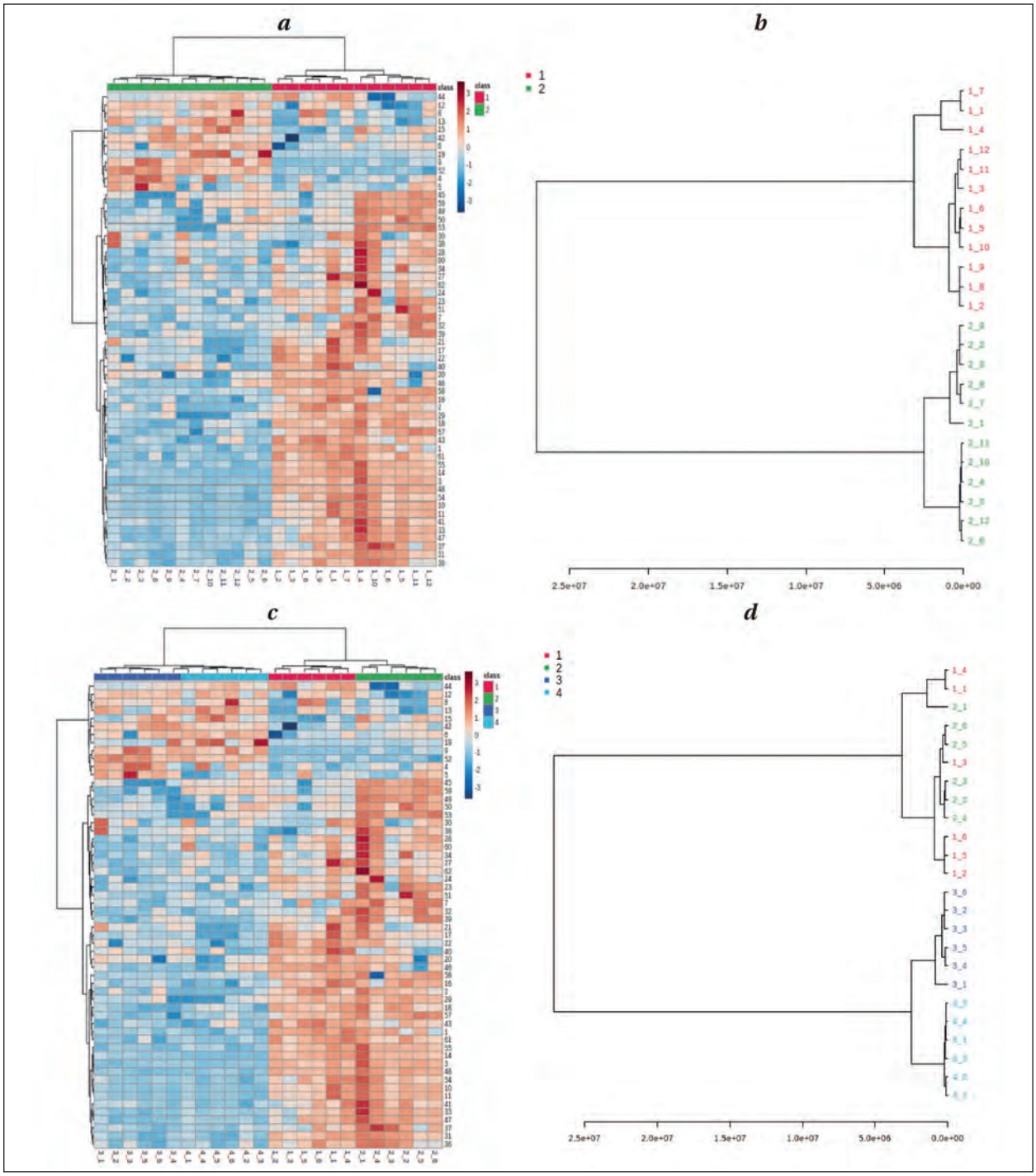

Fig. 6. Hierarchical cluster analysis of samples from the HILIC column.
Note. *a* — heat map of the studied metabolites of groups 1 and 2. The studied plasma samples by groups are arranged in the columns. Red color indicated group 1, green — group 2, and the identified component variables are arranged in rows. The colors range from blue to red, indicating a change in the content of the variables from very low (dark blue) to high (dark red). *b* — Dendrogram showing samples forming distinct clusters of groups 1 (red) and 2 (green). *c* — heat map of metabolites for comparison of daytime and nighttime sampling of the group: red corresponds to group 1 with the daytime sampling, green — to the group 1 with the nighttime sampling; dark blue represents group 2 with the daytime sampling, blue color shows group 2 with nighttime sampling, and the identified component variables are arranged in rows. The colors range from dark blue to dark red, indicating a change in the content of the variables from very low (dark blue) to high (dark red). *d* — dendrogram: 1 — group 1, daytime sampling; 2 — group 1, nighttime sampling; 3 — group 2, daytime sampling; 4 — group 2, nighttime sampling. Samples form clusters of groups 1 and 2, daytime and nighttime sampling.

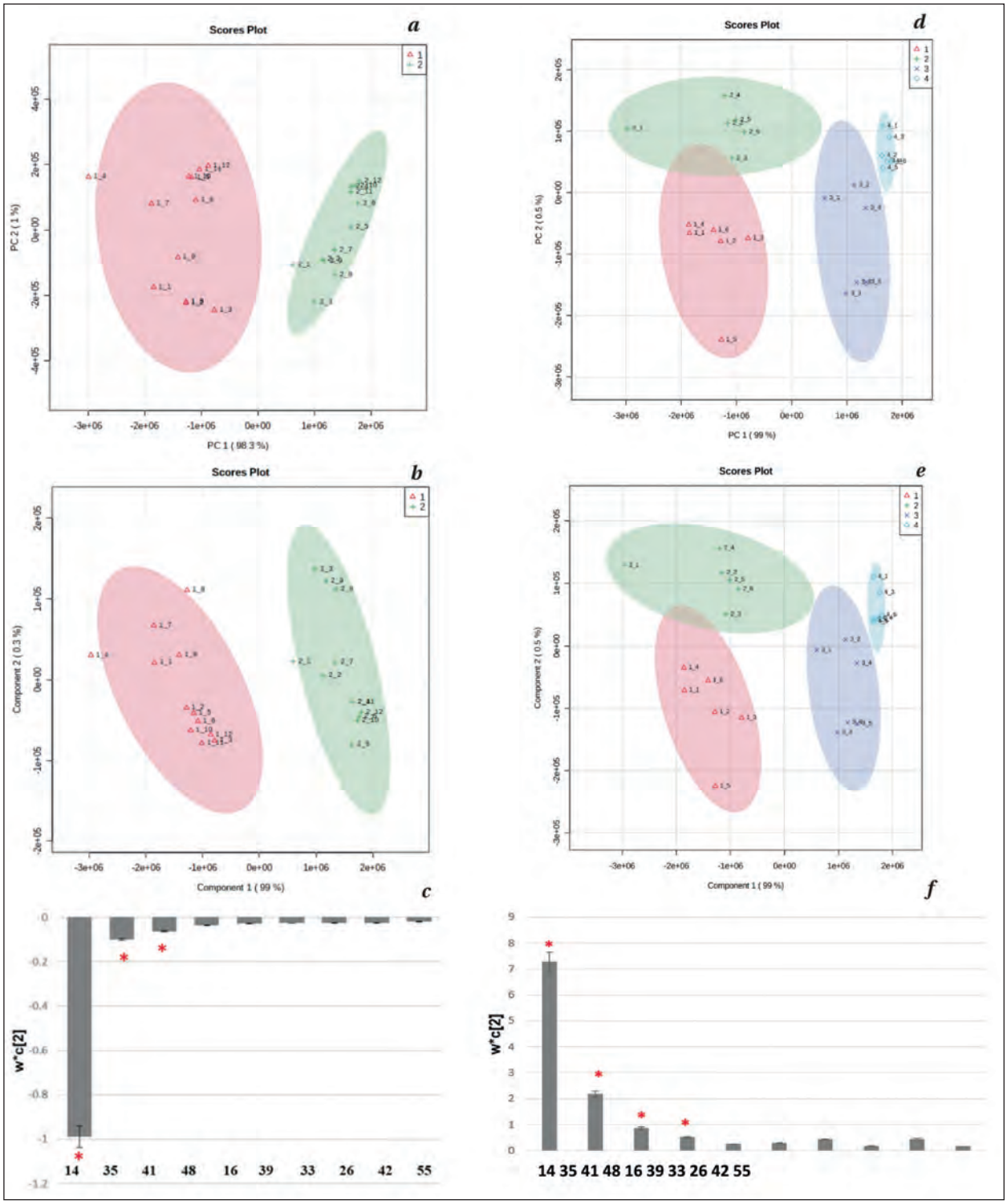

Fig. 7. Graphs of PCA (A) and PLS-DA (B) of groups 1 and 2 (HILIC).
Note. Group 1 cluster is represented by red cloud, Group 2 cluster is represented by green cloud. *a* — studied plasma samples of patients in group 1; *b* — studied plasma samples of patients in group 2. *c* — PLS-DA model loading plot, PC 2 (w*c [2]): each column represents the putative marker metabolite with standard errors displayed on the error panel. PCA (*d*) and PLS-DA (*e*) plots of differences between samples of daytime and nighttime sampling in groups 1 and 2 from column C18: red cloud, daytime sampling from group 1; green cloud, nighttime sampling from group 1; blue cloud, daytime sampling from group 2; blue cloud, nighttime sampling from group 2. Four separate clouds are formed, indicating significant differences both between groups and between samples at different times of the day. *f* — is the PLS-DA model loading plot, PC 2 (w*c [2]): each column represents the putative marker metabolite with standard errors displayed in the error panel.

clustering of samples both between and within the groups, depending on the time of sampling, with a slight overlap in the second component (Fig. 7, *d*). The PLS-DA model produced results similar to those of the PCA model (Fig. 7, *e*). Based on PLS-DA load plots (Fig. 7, *f*), we identified metabolites (at VIP > 0.5) that played a key role in intragroup differences, including 14 (m/z 162.1126, *Rt*=10.28, *P*=0.0201), 35 (m/z 780.5483, *Rt*=7.65, *P*<0.01), 41 (m/z 806.5649, *Rt*=7.58, *P*<0.01) and 48 (m/z 848.5354, *Rt*=7.65, *P*<0.01), whose levels were higher in Group 2 patient samples.

Discussion

As a result of non-targeted metabolome analysis of pooled plasma samples of patients in VS/UWS (group 1) and in MCS (group 2), we revealed several unidentified compounds, whose levels are most strongly associated with the type of cDoC (VS/UWS or MCS). To the best of our knowledge, this study was the first to compare «daytime» and «nighttime» plasma metabolome of patients with cDoC. Our findings have indicated significant differences between the studied samples, which suggests the possibility of identifying prognostic and diagnostic markers in the future research. However, it also became evident that non-targeted metabolomic analysis is not informative enough.

The first study on metabolomics in patients with cDoC was conducted by Jie Yu et al. in 2021 [21]. The authors used nontargeted and targeted plasma metabolome analysis in patients in VS/UWS and MCS to identify the main metabolomic abnormalities in patients of these two groups. Their findings showed that the metabolomic profile of patients with cDoC differed significantly not only from that of healthy volunteers, but also between patients in VS/UWS and MCS, with particularly relevant differences found in the lipidome analysis. The authors identified certain lipids whose levels were significantly elevated in patients in VS/UWS and MCS. For example, there was a significant difference in phosphatidylcholine and arachidonic acid levels between patients in VS/UWS and MCS, which, according to the authors, could serve as a marker for differential diagnosis of these disorders of consciousness. Also, significant differences in purine metabolism were observed in patients with cDoC compared to the control group of healthy volunteers. Patients in VS/UWS and MCS demonstrated decreased levels of adenosine, adenosine diphosphate, and adenosine monophosphate, which resulted from the adenosine triphosphate degradation. The results of other studies of metabolomics in patients with acute and subacute TBI have also shown that lipidomics was the most promising study [22, 23].

In a recently published paper by T. Dawiskiba et al addressing the metabolomic profile of patients diagnosed with brain death or coma, proline, orthophosphoric acid, β-hydroxybutyric acid, galactose, creatinine, valine, linoleic acid, arachidonic acid, medium-chain fatty acids were found to be both markers of acute traumatic brain damage and adverse outcome (death) predictors [24, 25]. Studies There are few studies on metabolomics in patients post hypoxic brain injury [26, 27]. Apparently, potential metabolomic markers in hypoxic damage would be those identified in ischemic stroke sych as lactate, pyruvate, glycolic acid, formate, glutamine, methanol, acetate, cysteine, folic acid, tyrosine, tryptophan, valine, carnitine, etc. [25, 28–30].

Thus, metabolomics is an rapidly evolving area of modern translational medicine [31–35]. Metabolomic changes can be minor and consist in the abnormal ratios between various chemical compounds, however, it is possible to identify some completely new chemical compounds («disease biomarkers») and/or loss of certain molecules normally present in the homeostatic state [36-38]. We believe that the study of metabolomic changes in patients with cDoC is a promising approach and will allow to create prognostic and differential models for this complex category of patients. The next stage of our work will be to determine the structure of the identified compounds, to study their prognostic value and changes depending on circadian rhythm.

There were several limitations in this study. First, the patients received various pharmacological drugs, so we could not exclude their effect on the metabolomic profile. Second, the patients received various types of nutritional support using specialized formulas. The third limitation of the study was the small number of patients and various etiology of brain damage (traumatic brain injury or hypoxia), as well as the absence of a control group of healthy volunteers (due to unavailability of blood sampling from the jugular vein).

Conclusion

Thus, non-targeted metabolomic analysis confirmed the hypothesis of probable significant quantitative and qualitative differences in the composition of metabolites depending on the type of cDoC and the phase of the circadian rhythm. The study identified a set of metabolites which are potential biomarkers for differential diagnosis of VS/UWS and MCS including 4, 33, 6, 1 (in the reverse-phase column experiment) and 14, 35, 41, 48 (in the hydrophilic column experiment), based on their significant contribution to intergroup and intragroup differences. Therefore, the aim of further research is to identify and characterize the above mentioned metabolites.

References

1. *Piradov M.A., Suponeva N.A., Voznyuk I.A., Kondratyev A.N., Shchegolev A.V., Belkin A.A., Zaitsev O.S., Pryanikov I.V., Petrova M.V., Ivanova N.E., Gnedovskaya E.V., Ryabinkina Yu.V., Sergeev D.V., Iazeva E.G., Legostaeva L.A., Fufaeva E.V., Petrikov S.S.* Russian workgroup on chronic disorders of consciousness. [Chronic disorders of consciousness: terminology and diagnostic criteria. The results of the first meeting of the Russian Working Group for Chronic Disorders of Consciousness]. *Annals of clinical and experimental neurology.* 2020; 14(1): 5–16. DOI: 10.25692/ACEN.2020.1.1. [in Russ.].
2. *Giacino J.T.* The vegetative and minimally conscious states: consensus-based criteria for establishing diagnosis and prognosis. *NeuroRehabilitation.* 2004; 19 (4): 293–298. PMID: 15671583.
3. *Giacino J.T., Katz D.I., Schiff N.D., Whyte J., Ashman E.J., Ashwal S., Barbano R., Hammond F.M., Laureys S., Ling G.S.F., Nakase-Richardson R., Seel R.T., Yablon S., Getchius T.S.D., Gronseth G.S., Armstrong M.J.* Practice guideline update recommendations summary: Disorders of consciousness: Report of the Guideline Development, Dissemination, and Implementation Subcommittee of the American Academy of Neurology; the American Congress of Rehabilitation Medicine; and the National Institute on Disability, Independent Living, and Rehabilitation Research. *Neurology.* 2018; 91 (10): 450–460. DOI: 10.1212/WNL.0000000000005926. PMID: 30089618; PMCID: PMC6139814.
4. *Kondziella D., Bender A., Diserens K., van Erp W., Estraneo A., Formisano R., Laureys S., Naccache L., Ozturk S., Rohaut B., Sitt J.D., Stender J., Tiainen M., Rossetti A.O., Gosseries O., Chatelle C.* EAN panel on coma, disorders of consciousness. european academy of neurology guideline on the diagnosis of coma and other disorders of consciousness. *Eur J Neurol.* 2020 May; 27 (5): 741–756. DOI: 10.1111/ene.14151. PMID: 32090418.
5. *Luppi A.I., Cain J., Spindler L.R.B., Górska U.J., Toker D., Hudson A.E., Brown E.N., Diringer M.N., Stevens R.D., Massimini M., Monti M.M., Stamatakis E.A., Boly M.* & *Curing Coma Campaign and Its Contributing Collaborators.* Mechanisms underlying disorders of consciousness: bridging gaps to move toward an integrated translational science. *Neurocrit Care.* 2021; 35 (Suppl 1): 37–54. DOI: 10.1007/s12028-021-01281-6. PMID: 34236622; PMCID: PMC8266690.
6. *Iliff J.J., Wang M., Liao Y., Plogg B.A., Peng W., Gundersen G.A., Benveniste H., Vates G.E., Deane R., Goldman S.A., Nagelhus E.A., Nedergaard M.* A paravascular pathway facilitates CSF flow through the brain parenchyma and the clearance of interstitial solutes, including amyloid β. *Science Translational Medicine.* 2012; 4 (147): 147ra111. DOI: 10.1126/scitranslmed.3003748.
7. *Kondratiev A.N., Tsentsiper L.M.* The glymphatic system of the brain: structure and practical significance. *Russian Journal of Anaesthesiology and Reanimatology.* 2019; 6: 72–80. DOI 10.17116/anaesthesiology201906172
8. *Lundgaard I., Lu M.L., Yang E., Peng W., Mestre H., Hitomi E., Deane R., Nedergaard M.* Glymphatic clearance controls state-dependent changes in brain lactate concentration. *Journal of Cerebral Blood Flow and Metabolism.* 2017; 37 (6): 2112–2124. DOI: 10.1177/ 0271678X16661202. PMID: 27481936 PMCID: PMC5464705.
9. *Lundgaard I., Li B., Xie L., Kang H., Sanggaard S., Haswell J.D.R., Sun W., Goldman S., Blekot S., Nielsen M., Takano T., Deane R., Nedergaard M.* Direct neuronal glucose uptake heralds activity-dependent increases in cerebral metabolism. *Nature Communications.* 2015; 6: 7807. DOI: 10.1038/ncomms7807.
10. *Hayton S., Maker G.L., Mullaney I., Trengove R.D.* Experimental design and reporting standards for metabolomics studies of mammalian cell lines. *Cell Mol Life Sci* 2017; 74 (24): 4421–4441. DOI: 10.1007/s00018-017-2582-1. PMID: 28669031.
11. *Fukuda A.M., Badaut J.* Aquaporin 4: a player in cerebral edema and neuroinflammation. *J Neuroinflammation.* 2012; 9: 279. DOI: 10.1186/ 1742-2094-9-279 PMCID: PMC3552817. PMID: 23270503.
12. *Gonzalez-Riano C., Saiz J., Barbas C., Bergareche A., Huerta J.M., Ardanaz E., Konjevod M., Mondragon E., Erro M.E., Chirlaque M.D., Abilleira E., Goñi-Irigoyen F., Amiano P.* Prognostic biomarkers of Parkinson's disease in the Spanish EPIC cohort: a multiplatform metabolomics approach. *npj Parkinsons Dis.* 2021; 7 (1): 73 (2021). DOI: 10.1038/s41531-021-00216-4. PMID: 34400650. PMCID: PMC8368017.
13. *Qureshi M.I., Vorkas P.A., Coupland A.P., Jenkins I.H., Holmes E., Davies A.H.* Lessons from metabonomics on the neurobiology of stroke. *Neuroscientist.* 2017; 23 (4): 374–382. DOI: 10.1177/1073858416673327. PMID: 28345376.
14. *Zheng F., Zhou Y.T, Li P.F., Hu E., Li T., Tang T., Luo J.K., Zhang W., Ding C.S., Wang Y.* Metabolomics analysis of hippocampus and cortex in a rat model of traumatic brain injury in the subacute phase. *Front Neurosci.* 2020; 14: 876. DOI: 10.3389/fnins.2020.00876. PMID: 33013291. PMCID: PMC7499474.
15. *Szpigel A., Hainault I., Carlier A., Venteclef N., Batto A.F., Hajduch E., Bernard C., Ktorza A., Gautier J.F., Ferré P., Bourron O., Foufelle F.* Lipid environment induces ER stress, TXNIP expression and inflammation in immune cells of individuals with type 2 diabetes. *Diabetologia.* 2018; 61 (2): 399–412. DOI: 10.1007/s00125-017-4462-5. PMID: 28988346.
16. *Eberlin L.S., Gabay M., Fan A.C., Gouw A.M., Tibshirani R.J., Felsher D.W., Zare R.N.* Alteration of the lipid profile in lymphomas induced by MYC overexpression. *Proc Natl Acad Sci USA.* 2014; 111 (29): 10450–10455. DOI: 10.1073/pnas.1409778111. PMCID: PMC4115527. PMID: 24994904.
17. *Chen M., Zhang J., Sampieri K., Clohessy J.G., Mendez L., Gonzalez-Billalabeitia E., Liu X.S., Lee Y.R., Fung J., Katon J.M., Menon A.V., Webster K.A., Ng C., Palumbieri M.D., Diolombi M.S., Breitkopf S.B., Teruya-Feldstein J., Signoretti S., Bronson R.T., Asara J.M., Castillo-Martin M., Cordon-Cardo C., Pandolfi P.P.* An aberrant SREBP-dependent lipogenic program promotes metastatic prostate cancer. *Nat Genet.* 2018; 50 (2): 206–218. DOI: 10.1038/s41588-017-0027-2. PMID: 29335545. PMCID: PMC6714980.

18. *Xiong N., Gao X., Zhao H., Cai F., Zhang F.C., Yuan Y., Liu W., He F., Zacharias L.G., Lin H., Vu H.S., Xing C., Yao D.X., Chen F., Luo B., Sun W., DeBerardinis R.J., Xu H., Ge W.P.* Using arterial-venous analysis to characterize cancer metabolic consumption in patients. *Nat Commun*. 2020; 11 (1): 3169. DOI: 10.1038/s41467-020-16810-8. PMID: 32576825. PMCID: PMC7311411.
19. *Chong J., Wishart D.S., Xia J.* Using Metaboanalyst 4.0 for comprehensive and integrative metabolomics data analysis. *Current Protocols in Bioinformatics*. 2019; 68 (1): e86. DOI: 10.1002/cpbi.86. PMID: 31756036.
20. *Xia J., Wishart D.S.* Metabolomic data processing, analysis, and interpretation using metaboanalyst. *Current Protocols in Bioinformatics*. 2011; 34 (1): 14.10.1–14.10.48. DOI: 10.1002/0471250953.bi1410s34.
21. *Yu J., Meng F., He F., Chen F., Bao W., Yu Y., Zhou J., Gao J., Li J., Yao Y., Ge W.P., Luo B.* Metabolic abnormalities in patients with chronic disorders of consciousness. *Aging and disease*. 2021; 12 (2): 386–403. DOI: 10.14336/AD.2020.0812.
22. *Proitsi P., Kim M., Whiley L., Simmons A., Sattlecker M., Velayudhan L., Lupton M.K., Soininen H., Kloszewska I., Mecocci P., Tsolaki M., Vellas B., Lovestone S., Powell J.F., Dobson R.J.B., Legido-Quigley C.* Association of blood lipids with Alzheimer's disease: a comprehensive lipidomics analysis. *Alzheimers Dement*, 2017; 13 (2): 140–151. DOI: 10.1016/j.jalz.2016.08.003. PMID: 27693183.
23. *Chitturi J., Li Y., Santhakumar V., Kannurpatti S.S.* Early behavioral and metabolomic change after mild to moderate traumatic brain injury in the developing brain. *Neurochem Int*. 2018; 120: 75–86. DOI: 10.1016/ j.neuint.2018.08.003. PMID: 30098378. PMCID: PMC6257993.
24. *Zheng F., Xia Z.A., Zeng Y.F., Luo J.K., Sun P., Cui H.J., Wang Y., Tang T., Zhou Y.T.* Plasma metabolomics profiles in rats with acute traumatic brain injury. *PLoS One*. 2017; 12 (8), e0182025. DOI: 10.1371/ journal.pone.0182025. PMID: 28771528. PMCID: PMC5542452.
25. *Dawiskiba, T., Wojtowicz, W., Qasem, B., Tukaszewski M., Mielko K.A., Dawiskiba A., Banasik M., Skóra J.P., Janczak D., Młynarz P.* Brain-dead and coma patients exhibit different serum metabolic profiles: preliminary investigation of a novel diagnostic approach in neurocritical care. *Sci Rep*. 2021; 11 (1): 15519. DOI: 10.1038/s41598-021-94625-3. PMID: 34330941. PMCID: PMC8324823.
26. *Tsai I.L., Kuo T.C., Ho T.J., Harn Y.C., Wang S.Y., Fu W.M., Kuo C.H., Tseng Y.J.* Metabolomic dynamic analysis of hypoxia in MDA-MB-231 and the comparison with inferred metabolites from transcriptomics data. *Cancers (Basel)*. 2013; 5 (2): 491–510. DOI: 10.3390/ cancers5020491. PMCID: PMC3730319. PMID: 24216987.
27. *Solberg R., Kuligowski J., Pankratov L., Escobar J., Quintás G., Lliso I., Sánchez-Illana A., Saugstad O.D., Vento M.* Changes of the plasma metabolome of newly born piglets subjected to postnatal hypoxia and resuscitation with air. *Pediatr Res*. 2016; 80 (2): 284–292. DOI: 10.1038/pr.2016.66. PMID: 27055187.
28. *Baranovicova E., Grendar M., Kalenska D., Tomascova A., Cierny D., Lehotsky J.* NMR metabolomic study of blood plasma in ischemic and ischemically preconditioned rats: an increased level of ketone bodies and decreased content of glycolytic products 24 h after global cerebral ischemia. *J. Physiol. Biochem*. 2018; 74 (3): 417–429. DOI: 10.1007/ s13105-018-0632-2. PMID: 29752707.
29. *Liu P., Li R., Antonov A.A., Wang L., Li W., Hua Y., Guo H., Wang L., Liu P., Chen L., Tian Y., Xu F., Zhang Z., Zhu Y., Huang Y.* Discovery of metabolite biomarkers for acute ischemic stroke progression. *J. Proteome Res*. 2017; 16 (2): 773–779. DOI: 10.1021/acs.jproteome.6b00779. PMID: 28092160.
30. *Wang D., Kong J., Wu J., Wang X., Lai M.* GC–MS-based metabolomics identifies an amino acid signature of acute ischemic stroke. *Neurosci. Lett*. 2017; 642: 7–13. DOI: 10.1016/j.neulet.2017.01.039 PMID: 28111353.
31. *Wang Y., Wang Y. G., Ma T. F., Li M., Gu S. L.* Dynamic metabolites profile of cerebral ischemia/reperfusion revealed by (1)H NMR-based metabolomics contributes to potential biomarkers. *Int. J. Clin. Exp. Pathol*. 2014; 7 (7): 4067–4075. PMID: 25120785. PMCID: PMC4129020.
32. *Fiehn O.* Metabolomics: The link between genotypes and phenotypes. *Plant Mol. Biol*. 2002; 48 (1–2): 155–171. DOI: 10.1023/ A:1013713905833. PMID: 11860207.
33. *Wishart D.S., Feunang Y.D., Marcu A., Guo A.C., Liang K., Vázquez-Fresno R., Sajed T., Johnson D., Li C., Karu N., Sayeeda Z., Lo E., Assempour N., Berjanskii M., Singhal S., Arndt D., Liang Y., Badran H., Grant J., Serra-Cayuela A., Liu Y., Mandal R., Neveu V., Pon A., Knox C., Wilson M., Manach C., Scalbert A.* HMDB 4.0: The human metabolome database for 2018. *Nucleic Acids Res*. 2018; 46 (D1)D608–D617. DOI: 10.1093/nar/gkx1089. PMID: 29140435. PMCID: PMC5753273.
34. *Dryagina N.V., Kondratieva E.A., Dubrovsky Ya.A., Kondratiev A.N.* The brain metabolome. *Russian Neurological Journal*. 2020; 25 (1): 4–12. DOI 10.30629/2658-7947-2020-25-1-4-12
35. *Lokhov P. G., Lisitsa A.V., Archakov A. I.* Metabolomic blood test: purpose, implementation, and interpretation of data. *Biomedical chemistry / Biomeditsinskaya khimiya*. 2017; 63 (3): 232–240. DOI: 10.18097/PBMC20176303232. PubMed: 28781256 http://pbmc.ibmc.msk.ru/ru/article-ru/PBMC-2017-63.
36. *Chernevskaya E.A., Beloborodova N.V.* Gut Microbiome in Critical Illness (Review). *General Reanimatology*. 2018; 14 (5): 96–119. DOI: 10.15360/1813-9779-2018-5-96-119.
37. *Nicholson J.K., Lindon J.C., Holmes E.* «Metabonomics»: understanding the metabolic responses of living systems to pathophysiological stimuli via multivariate statistical analysis of biological NMR spectroscopic data. *Xenobiotica*. 1999; 29 (11): 1181–1189. DOI: 10.1080/004982599238047. PMID: 10598751.
38. *Nicholson J.K., Holmes E., Kinross J.M., Darzi A.W., Takats Z., Lindon J.C.* Metabolic phenotyping in clinical and surgical environments. *Nature*. 2012; 491 (7424): 384–392. DOI: 10.1038/nature11708. PMID: 23151581.

39. *Fiehn O.* Metabolomics: The link between genotypes and phenotypes. *Plant Mol. Biol.* 2002; 48 (1–2): 155–171. DOI: 10.1023/A: 1013713905833. PMID: 11860207.
40. *Trifonova O.P., Maslov D.L., Balashova E.E., Lokhov P.G.* Mass spectrometry-based metabolomics diagnostics — myth or reality? *Expert Review of Proteomics.* 2021; 18: 7–12. DOI: 10.1080/14789450.2021.1893695.

Received 13.11.2021
Accepted 13.12.2021